Climate impact of aircraft-induced cirrus assessed from satellite observations before and during COVID-19

Johannes Quaas, Edward Gryspeerdt, Robert Vautard, Olivier Boucher

ENVIRONMENTAL RESEARCH
LETTERS

LETTER • OPEN ACCESS

Climate impact of aircraft-induced cirrus assessed from satellite observations before and during COVID-19

IOP Publishing Environ. Res. Lett. 16 (2021) 064051 https://doi.org/10.1088/1748-9326/abf686

ENVIRONMENTAL RESEARCH
LETTERS

OPEN ACCESS

RECEIVED
26 November 2020

REVISED
15 March 2021

ACCEPTED FOR PUBLICATION
9 April 2021

PUBLISHED
2 June 2021

LETTER

Climate impact of aircraft-induced cirrus assessed from satellite observations before and during COVID-19

Johannes Quaas[1,*], **Edward Gryspeerdt**[2], **Robert Vautard**[3] and **Olivier Boucher**[3]

[1] Institute for Meteorology, Universität Leipzig, Leipzig, Germany
[2] Space and Atmospheric Physics Group, Imperial College London, London, United Kingdom
[3] Institut Pierre-Simon Laplace, Sorbonne Université/CNRS, Paris, France
[*] Author to whom any correspondence should be addressed.

E-mail: johannes.quaas@uni-leipzig.de

Keywords: aviation-induced cirrus, aviation climate forcing, COVID-19

Supplementary material for this article is available online

Abstract

Aircraft produce condensation trails, which are thought to increase high-level cloudiness under certain conditions. However the magnitude of such an effect and whether this contributes substantially to the radiative forcing due to the aviation sector remain uncertain. The very substantial, near-global reduction in air traffic in response to the COVID-19 outbreak offers an unprecedented opportunity to identify the anthropogenic contribution to the observed cirrus coverage and thickness. Here we show, using an analysis of satellite observations for the period March–May 2020, that in the 20% of the Northern Hemisphere mid-latitudes with the largest air traffic reduction, cirrus fraction was reduced by $\sim 9 \pm 1.5\%$ on average, and cirrus emissivity was reduced by $\sim 2 \pm 5\%$ relative to what they should have been with normal air traffic. The changes are corroborated by a consistent estimate based on linear trends over the period 2011–2019. The change in cirrus translates to a global radiative forcing of 61 ± 39 mW m^{-2}. This estimate is somewhat smaller than previous assessments.

1. Introduction

The fact that aviation leads to condensation trails (or contrails) that may create artificial cirrus and potentially alter naturally occurring cirrus has been well documented [1–3]. The former occurs through the spreading of line-shaped contrails into larger, amorphous cirrus while the latter is due to dehydration of the upper atmosphere and the impact of the emitted aerosol on the cirrus properties. However, quantifying the global radiative impact of such a perturbation is proving to be challenging. In a modeling study, Burkhardt and Kärcher [4] quantified the fractional coverage of aviation-induced cirrus for the year 2002 at 1%–4% in regions that experience a large amount of air traffic, mainly over Europe, Western North America, and the North Atlantic Ocean. The associated global radiative forcing was estimated in their study at 38 mW m^{-2} for 2002. Assuming the forcing scales with air traffic, it would be about 86 mW m^{-2} in the year 2019 given a growth rate of approximately 5% per year [5], see supplementary material (available online at stacks.iop.org/ERL/16/064051/mmedia). In a refined study using a more complex cloud scheme, Bock and Burkhardt [6] revised this estimate to 56 mW m^{-2} for 2006, implying a forcing of 106 mW m^{-2} in 2019. Although they are based on physical processes, such models remain very difficult to validate against observations. Also, the model does not necessarily include all mechanisms by which aircraft impacts high-level cloudiness.

Boucher [7] used synoptic cloud reports from land and ship stations to detect a positive trend in cirrus occurrence and a negative trend in cloud amount in the presence of cirrus over air traffic corridors. However their analysis was restricted to a 10 year period as the database was discontinued. Satellite data have also been used to quantify the aviation impact on cirrus. Tesche *et al* [8] found an increase in cirrus optical depth in satellite lidar observations in portions of the satellite track that were crossed by aircraft in comparison to neighboring control conditions. Stordal *et al* [9] correlated trends in cirrus cover with aircraft density data and obtained a noisy signal

from which they estimate a regional increase in cloud cover by 1%–2% attributable to aircraft, and estimated a radiative forcing of 30 mW m^{-2} in the period 1992–1999 vs 1984–1991.

A common problem to trend analyses is that multiple influences on cirrus, including global warming and natural decadal variability, may also act as confounding factors. For similar reasons it is difficult to compare regions inside and outside air traffic corridors. Temporary reductions in air traffic thus offer exceptional conditions to test the hypothesis of an impact of aviation on the cirrus cover. The grounding of air traffic over the USA after the 9/11 terrorist attacks offered such an opportunity. One study postulated an effect of the absence of contrails on the diurnal temperature range [10] but it has been later called into question [11, 12]. Indeed the shutdown lasted only a few days and the observed changes were largely consistent with the meteorological situation after 9/11.

The COVID-19 pandemic is exceptional in comparison to previous air traffic shutdowns in that the reduction in the number of flights is very substantial (about 70% in large regions, supplementary figure S1), over a long period of time (several months) and at a near-global scale. This provides an unprecedented opportunity to infer causality between air traffic and cirrus cloudiness. The key obstacle to the statistical analysis is that cirrus amount and properties are highly variable in space and time and bear interannual variability even when considering 3 month period averages. On such a timescale, cirrus cover—which is largely controlled by the weather—may deviate substantially from its long-term climatology even in absence of air traffic change. In order to account for such variability, we define atmospheric circulation analogues by finding meteorological situations in the months of March to May of years 2011–2019 that match the circulation situation at each location and for each day in the March–May 2020 period (see supplementary material for details). Observed 2020 cirrus are then compared to what they have been in other years under those regional circulation analogues. Contrail cirrus clouds form in synoptic situations favoring large ice super-saturation areas [13]. Circulation analogues have been largely used in extreme event attribution studies in order to disentangle thermodynamical and dynamical contributions of climate change to the change in intensity or probability of occurrence of climate extremes [14, 15]. They allow to estimate various kinds of statistics conditioned to regional circulation.

This study focuses on the Northern Hemisphere mid-latitudes from 27° N to 68° N where a large fraction of the world air traffic takes place. The difference (2019 minus 2020) in flight track density is considered for each day and 1° × 1° grid-box (figure S1) and classified in quintiles spanning the entire domain and period. The smallest differences correspond to regions unaffected by air traffic and, consequently, by its reduction in 2020.

The first quintile can thus serve as control conditions. Large differences in flight density correspond to regions where aviation has the largest potential to affect cirrus. Small differences tend to occur in early to mid-March 2020, when much of the international air traffic was still active, while large differences occur from mid-March onwards. The reason for considering only quintiles of the distribution and for transforming the space-time domain to a flight-track-density-difference coordinate is that it allows broadening the statistics and suppressing the large weather noise. However, it comes at the expense that more subtle factors that may also influence the aircraft impact on cirrus [16, 17] are not controlled for.

2. Results

We use satellite retrievals from the moderate resolution imaging spectroradiometer (MODIS) [18]; on board the Aqua and Terra satellites from which we extract a cirrus cloud cover (cloud horizontal extent) and cirrus effective emissivity as a measure of their opacity (see supplementary material). The cirrus fraction for each grid-box and each day in March–May 2020 is classified according to the difference in flight track density (figure 1).

Statistics of the cirrus fraction in analogue circulation conditions over the March–May 2011–2019 period, as well as of the March–May 2011–2019 climatology, are also shown. Mean values for cirrus fractional cover are substantially larger than medians (figure S2), indicating that the distribution is skewed at the 1° × 1° resolution considered here, with occasionally large, but predominantly smaller fractional cirrus cover.

However, the results for means and medians are largely consistent. The fractional covers show differences of the order of ±1% for the four overpass times (two during day and two during night, variability shown by the vertical bars) both in terms of mean and median, and about ±2% for the cirrus emissivity. There is some systematic variability in cirrus cover and emissivity (opacity) between the different flight track density change quintiles, with somewhat lower cirrus coverage and also emissivity in the middle three flight track density change quintiles. This is attributable to the fact that these quintiles reflect different regions (figure S1). The diurnal cycle in cirrus fraction is small (figure S3), with slightly more cirrus during day than during night. It is more pronounced for emissivity—cirrus are least opaque in the evening and thickest in the night in our results.

Cirrus statistics in the first quintile (control conditions) are systematically closer to each other for 2020 and the circulation analogues than they are

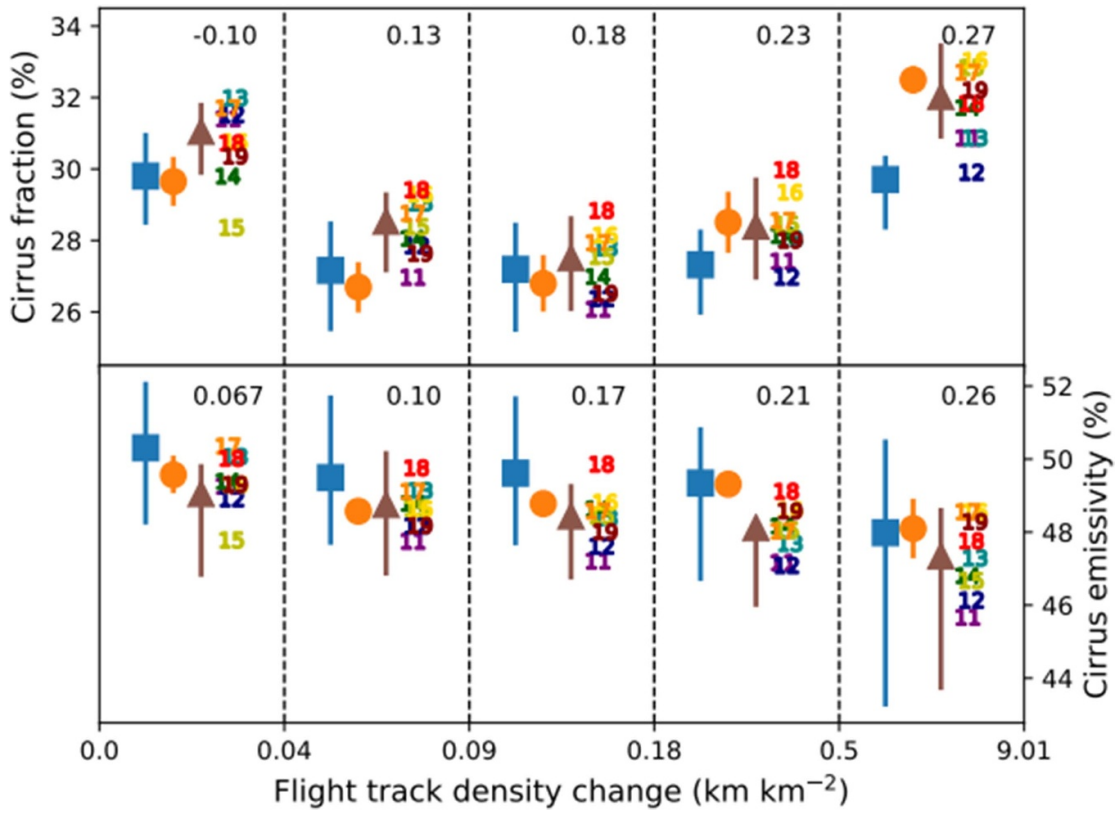

Figure 1. Cirrus fraction and emissivity as a function of flight track density change between 2020 and 2019 in the midlatitudes of the Northern Hemisphere. Cirrus fraction (top) and emissivity (bottom) from daily level-3 (1° × 1°) MODIS retrievals, both expressed in percent, as a function of quintiles of the difference in flight track density, for grid-boxes containing cirrus. The mean of the spatio-temporal distribution of the 1° × 1° grid-boxes in the region 27° to 68° N is shown. Both MODIS-Terra (approximate overpass times 10.30 a.m. and 10.30 p.m.) and MODIS-Aqua (overpass times 1.30 a.m. and 1.30 p.m.) data are considered. Blue squares—March–May 2020; orange circles—circulation analogues March–May 2011–2019; brown triangles—climatology March–May 2011–2019. Also the March–May means for each year, averaged for all four satellite overpasses, are provided, color coded from purple (2011 marked as 11) to dark red (2019 marked as 19). The numbers in the top right for each quintile show the linear trends 2011–2019 (% yr^{-1}), as absolute percent changes. The vertical bars show the range spanned by the four satellite overpass times.

for 2020 and the climatology, showing the ability of the circulation analogues to capture circulation-conditioned cirrus statistics. This shows that 2020 circulation conditions are less conducive to cirrus formation than the climatological conditions at least in the control quintile. However, the differences between 2020 and the circulation analogues are larger for cirrus emissivity (opacity) (figure 1) than for cirrus fraction in the control quintile. This is because while cirrus occurrence is largely driven by large-scale meteorological conditions, its optical properties are also a strong function of microphysical processes that more closely relate to small to mesoscale vertical wind and to aerosol concentrations [19]. This larger emissivity in regions unaffected by air traffic change in 2020 can be contrasted by a lack of positive anomaly in the regions with large change in flight track density. Note there is some positive trend in emissivity in particular in the upper quintiles (see below).

We diagnose an average net effect in cirrus properties attributable to air traffic by computing the difference between 2020 and analogues relative to their difference under the control conditions (figure 2). Both cirrus coverage and emissivity show a decrease with decreasing air traffic. The difference between areas affected by aviation and those not affected as diagnosed here includes all mechanisms, i.e. contrails, contrail-induced cirrus, and near-field modifications of cirrus by the impact of aviation aerosol emissions. This also includes a contrail buffering effect through the depletion of naturally occurring cirrus in the presence of aircraft-induced cirrus [4]. Besides aircraft, surface aerosol emissions were also reduced during the COVID-19 shutdown. To the extent that aerosol emissions are related to CO_2 emissions, substantial emission reductions would be expected [20]. However, observations of column aerosol concentrations were not found to differ systematically from the climatology even over regions strongly affected by emissions reductions [21, 22]. Furthermore there is no reason to expect surface emission changes to project preferably on aircraft corridors after long-range transport to the upper troposphere. Therefore we expect the observed changes to represent a substantial fraction of aircraft impacts on high-level cloudiness.

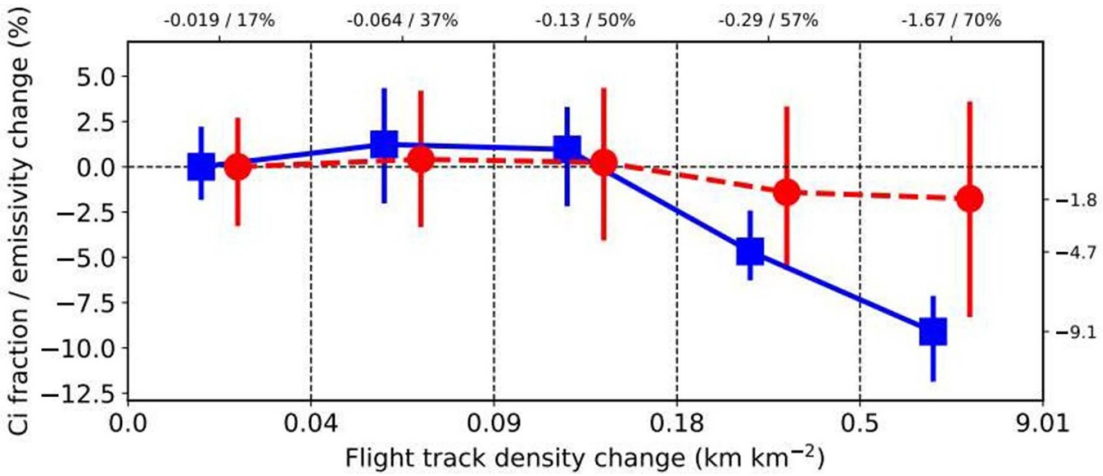

Figure 2. Cirrus fraction and emissivity decrease as flight track density change increases when computed for similar weather conditions. Mean relative difference in cirrus fraction (blue squares) and cirrus emissivity (red circles) between March–May 2020 and March–May in analogue circulations 2011–2019, expressed as the deviation from zero aviation change (lowest quintile), as a function of flight track density change 2019 minus 2020. The vertical bars show the full range spanned by the four satellite overpasses. The labels on the top indicate the average change in flight track density within each quintile in absolute and in relative numbers.

In the uppermost quintile of flight track density difference, the cirrus cover was reduced by more than 9% relative to the cirrus cover in analogues, and the emissivity of these clouds was decreased by almost 2%. The change in emissivity was not clearly distinct from zero; it accounts for changes in cirrus thickness where aircraft aerosol emissions impact cirrus, and a shift in the distribution of emissivity due to aircraft-induced cirrus and contrails. Two factors have to be accounted for when estimating the cirrus cover response to all aircraft: (a) flight track density on average was only reduced by 70% in the fifth quintile, and (b) there was an increase in air traffic throughout the reference period. We approximate this increase by accounting for a 5% growth rate per year [5] between the middle of the 2011–2019 reference period and the year 2019 for which we estimate the cirrus change. This corresponds to 21% for four and a half years, implying that the 2019 air traffic is 121% of what was observed on average during the reference period. Together, this implies that 17% of the cirrus in 2019 in the region corresponding to the fifth quintile are due to air traffic (see also figure S4 for further explanation).

This estimate is consistent with an independent estimate: The aircraft impact on cirrus can also be derived from the trend over the 2011–2019 period in the upper quintile (+0.27% per year, statistically significant at the 99% confidence level using a one-sided probability p of the Student t-distribution). For this quintile with the largest air traffic impact, the cirrus coverage was substantially lower in the early part of the period compared to the more recent one. The two quintiles with statistically significant trends are the fourth (+0.23% per year) and the fifth, whereas quintiles 1–3 do not show significant trends. We posit that the trends in the upper quintiles of flight track density change are due to air traffic as the regions of large flight track density difference are also those which have experienced an increase in air traffic. For the fifth quintile area, the trend in cirrus cover implies an increase by 0.27% yr^{-1} × 9 yr = 2.4% over the nine years analyzed, and at the same time, air traffic increased by 5% yr^{-1}, i.e. by 48%. This implies that 2.4%/0.48 = 5% absolute or 16% of the average cirrus cover of 0.32 are attributable to air traffic. This trend analysis thus corroborates the quantitative estimate from the COVID-19 period and the two arguments together provide strong evidence for a causal link between air traffic and cirrus coverage, as cirrus coverage qualitatively and quantitatively consistently responds to the long-term increase as well as to the rapid decrease in aviation activity. Similarly, there is also a positive trend in emissivity which is also present in the lowest quintiles but increases in magnitude in the upper quintiles. These trends could in principle also stem from other causes, including a trend attributable to global warming, natural variability, or to a drift in satellite instrument calibration. However, the fact that the trends show a systematically different behavior for the quintiles in air traffic reduction hints at air traffic begin the cause for the observed trends.

There is little diurnal cycle in the response of cirrus fraction (figure S3), changes are somewhat more pronounced at late evening and morning. A possible explanation is in the diurnal cycle of air traffic, which is larger in the mornings and evenings than at early afternoon for intercontinental flights but also many intra-continental ones.

The radiative forcing implied by the results shown in figure 2 is computed using radiative transfer

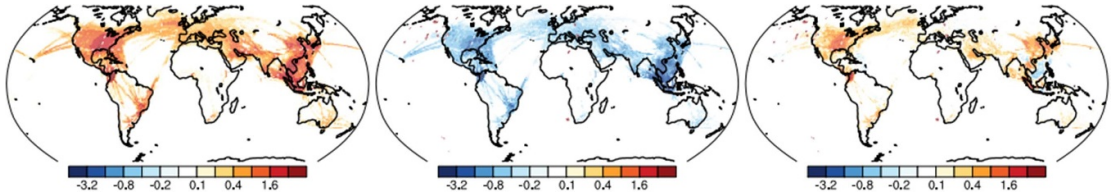

Figure 3. Radiative forcing (W m^{-2}) due to aviation-induced cirrus in March–May 2019. Left: terrestrial (longwave) spectrum, middle: solar (shortwave spectrum), right: net radiative forcing.

modeling (see supplementary material). The radiative fluxes are computed for weather conditions sampled throughout March–May 2019, and the changes in high cloud extent and opacity are estimated from the 2019 flight track distributions, imposing the changes where the flight track density was within the upper two quintiles of the track density changes in figure 2. Note that although some of the cirrus clouds are too thin to be detected by MODIS [23, 24], they are considered for their radiative impact, by changing them in the computation in the radiative flux perturbation in the same way as those diagnosed in figure 2. The resulting geographical distribution in difference 2019 vs 2020 in cirrus coverage is shown in figure S5. The results are shown in figure 3 in terms of radiative forcing. The forcing due to all aviation, not just the change 2019–2020 is estimated using the fraction of flights still active in 2020 and the trend in aviation within the reference period (see supplementary material and figure S4). The estimate further accounts for a systematic underestimation of the forcing in climate model radiation codes [3] and a small systematic difference between March–May and annual mean forcings (see supplementary material). The radiative forcing due to the aviation-induced cirrus for March–May of the year 2019 is estimated to be +227 mW m^{-2} in the terrestrial (longwave) spectrum in the global average, of which 165 mW m^{-2} are balanced by a cooling effect in the solar (shortwave) spectrum. The share of the shortwave forcing, that offsets about 70% of the longwave forcing, is larger than what was found in previous studies [6, 25, 26], partly owing to the increase in emissivity that also impacts the cirrus albedo. In particular over Europe, the effects in the solar and terrestrial spectra nearly cancel to yield a net small forcing. The net forcing is substantially positive, however, over eastern North America and East Asia. The net radiative forcing in its global, March–May average, is estimated at +61 mW m^{-2}.

We estimate the uncertainty of this forcing estimate (see supplementary material), which is dominated by the uncertainty due to the weather variability. The 2-σ range is assessed at ±64%. Model results by Chen and Gettelman [27] show that there is very little annual cycle in the global forcing due to contrail cirrus, the difference of 9% between annual-mean and March–May mean is factored into the assessment. Our results for March to May are thus comparable to annual-mean results published in other studies.

3. Discussion

Our estimate of the net RF of 61 ±39 mW m^{-2} that is based on the observations-derived aircraft impact on cirrus is somewhat lower than the estimate and 5%–95% confidence interval of 50 (20–150) mW m^{-2} given for the year 2011 (i.e. about 74 (30–222) mW m^{-2} for 2019 considering an annual increase by 5%) by the Intergovernmental Panel on Climate Change in the fifth assessment report [28], and substantially lower than the model-based estimates of Bock and Burkhardt [6]. It is also smaller than, but consistent considering the uncertainty ranges, with the estimate by Lee *et al* [3] that reviewed all available information including modeling. A large part of the difference appears to be due to our lower cirrus coverage attributable to air traffic, though Bock and Burkhardt also have a contribution from subvisible cirrus which the MODIS analysis may miss. The aviation impact derived from an analysis of cirrus trends in each quintile yields an estimate of aviation-induced cirrus that is very similar to the one obtained from the COVID-related traffic reduction, corroborating this result.

Data availability statement

The following data that support the findings of this study are openly available: MODIS satellite data, ERA5 and NCEP reanalysis data (see acknowledgements for details). The following data that support the findings of this study are available upon request from the authors: Flight track densities and circulation analogues.

The data that support the findings of this study are available upon reasonable request from the authors.

Acknowledgments

J Q received support from the EU Horizon2020 projects ACACIA (GA no. 875036) and FORCES

(GA no. 821205). O B and J Q further were supported by the EU Horizon2020 project CONSTRAIN (GA no. 820829). E G was supported by a Royal Society University Research Fellowship (URF/R1/191602). The MODIS cloud products MYD08_D3 from Aqua and MOD08_D3 from Terra were used in this study from the Atmosphere Archive and Distribution System (LAADS) Distributed Active Archive Center (DAAC), https://ladsweb.nascom.nasa.gov/. ERA5 data were obtained from the European Centre for Medium-range Weather Forecasts (ECMWF) archive, www.ecmwf.int/en/forecasts/datasets/reanalysis-datasets/era5. NCEP Reanalysis Derived data are provided by the NOAA/OAR/ESRL PSL, Boulder, Colorado, USA, from their Web site at https://psl.noaa.gov/. We would like to thank Jan Kretzschmar and Jonas Schaefer, Leipzig University, for support with the PRP analysis. Eulalie Boucher is acknowledged for the reconstruction of an air traffic distribution for 2019 and 2020 used in the initial phase of the study.

ORCID iDs

Johannes Quaas https://orcid.org/0000-0001-7057-194X
Edward Gryspeerdt https://orcid.org/0000-0002-3815-4756
Robert Vautard https://orcid.org/0000-0001-5544-9903
Olivier Boucher https://orcid.org/0000-0003-2328-5769

References

[1] Well E D 1919 Clouds formed by airplanes *Sci. Am.* **120** 601
[2] Haywood J M, Allan R P, Bornemann J, Forster P, Francis P N, Milton S, Rädel G, Rap A, Shine K P and Thorpe R 2009 A case study of the radiative forcing of persistent contrails evolving into contrail-induced cirrus *J. Geophys. Res.* **114** D24201
[3] Lee D S *et al* 2021 The contribution of global aviation to anthropogenic climate forcing for 2000–2018 *Atmos. Environ.* **244** 1–29
[4] Burkhardt U and Kärcher B 2011 Global radiative forcing from contrail cirrus *Nat. Clim. Change* **1** 54–8
[5] ICAO, International Civil Aviation Organization 2018 Annual Report 2018, The World of Air Transport in 2018 (www.icao.int/annual-report-2018/Documents/Annual.Report.2018_Air Transport Statistics.pdf)
[6] Bock L and Burkhardt U 2016 Reassessing properties and radiative forcing of contrail cirrus using a climate model *J. Geophys. Res. Atmos.* **121** 9717–36
[7] Boucher O 1999 Air traffic may increase cirrus cloudiness *Nature* **397** 30–1
[8] Tesche M, Achtert P, Glantz P and Noone K J 2016 Aviation effects on already-existing cirrus clouds *Nat. Commun.* **7** 12016
[9] Stordal F, Myhre G, Stordal E J G, Rossow W B, Lee D S, Arlander D W and Svendby T 2005 Is there a trend in cirrus cloud cover due to aircraft traffic? *Atmos. Chem. Phys.* **5** 2155–62
[10] Travis D J, Carleton A M and Lauritsen R G 2004 Regional variations in U.S. diurnal temperature range for the 11–14 September 2001 aircraft groundings: evidence of jet contrail influence on climate *J. Clim.* **17** 1123–34
[11] Dietmüller S, Ponater M, Sausen R, Hoinka K and Pechtl S 2008 Contrails, natural clouds, and diurnal temperature range *J. Clim.* **21** 5061–75
[12] Van Wijngaarden W A 2012 Examination of diurnal temperature range at coterminous U.S. stations during Sept. 8–17, 2001 *Theor. Appl. Climatol.* **109** 1–5
[13] Bier A, Burkhardt U and Bock L 2017 Synoptic control of contrail cirrus life cycles and their modification due to reduced soot number emissions *J. Geophys. Res.* **122** 11584–603
[14] Cattiaux J, Vautard R, Cassou C, Yiou P, Masson-Delmotte V and Codron F 2010 Winter 2010 in Europe: a cold extreme in a warming climate *Geophys. Res. Lett.* **37** L20704
[15] Vautard R, Yiou P, Otto F, Stott P, Christidis N, Van Oldenborgh G J and Schaller N 2016 Attribution of human-induced dynamical and thermodynamical contributions in extreme weather events *Environ. Res. Lett.* **11** 114009
[16] Burkhardt U, Bock L and Bier A 2018 Mitigating the contrail cirrus climate impact by reducing aircraft soot number emissions *npj Clim. Atmos. Sci.* **1** 37
[17] Bier A and Burkhardt U 2019 Variability in contrail ice nucleation and its dependence on soot number emissions *J. Geophys. Res.* **124** 3384–400
[18] Platnick S *et al* 2017 The MODIS cloud optical and microphysical products: collection 6 updates and examples from Terra and Aqua *IEEE Trans. Geosci. Remote Sens.* **55** 502–25
[19] Krämer M *et al* 2021 A microphysics guide to cirrus—part II: climatologies of clouds and humidity from observations *Atmos. Chem. Phys.* **20** 12569–608
[20] Le Quéré C *et al* 2020 Temporary reduction in daily global CO_2 emissions during the COVID-19 forced confinement *Nat. Clim. Change* **10** 647–53
[21] Diamond M S and Wood R 2020 Limited regional aerosol and cloud microphysical changes despite unprecedented decline in nitrogen oxide pollution during the February 2020 COVID-19 shutdown in China *Geophys. Res. Lett.* **47** e2020GL088913
[22] Le T, Wang Y, Liu L, Yang J, Yung Y L, Li G and Seinfeld J H 2020 Unexpected air pollution with marked emission reductions during the COVID-19 outbreak in China *Science* **369** 702–6
[23] Holz R E, Ackerman S A, Nagle F W, Frey R, Dutcher S, Kuehn R E, Vaughan M A and Baum B 2008 Global moderate resolution imaging spectroradiometer (MODIS) cloud detection and height evaluation using CALIOP *J. Geophys. Res.* **113** D00A19
[24] Kärcher B 2018 Formation and radiative forcing of contrail cirrus *Nat. Commun.* **9** 1824
[25] Duda D P *et al* 2019 Northern Hemisphere contrail properties derived from Terra and Aqua MODIS data for 2006 and 2012 *Atmos. Chem. Phys.* **19** 5313–30
[26] Myhre G *et al* 2009 Intercomparison of radiative forcing calculations of stratospheric water vapour and contrails *Meteorol. Z* **18** 585–96
[27] Chen C-C and Gettelman A 2013 Simulated radiative forcing from contrails and contrail cirrus *Atmos. Chem. Phys.* **13** 12525–36
[28] Boucher O *et al* 2013 Clouds and aerosols *Climate Change 2013: The Physical Science Basis. Contribution of Working Group I to the Fifth Assessment Report of the Intergovernmental Panel on Climate Change* ed T F Stocker, D Qin, G-K Plattner, M Tignor, S K Allen, J Boschung, A Nauels, Y Xia, V Bex and P M Midgley (Cambridge: Cambridge University Press)